Journal of Power Sources 189 (2009) 611–615

Contents lists available at ScienceDirect

Journal of Power Sources

journal homepage: www.elsevier.com/locate/jpowsour

Short communication

Synthesis and characterisation of iron tungstate anode materials

Emma Kendrick[a,b,*], Agata Świątek[a], Jerry Barker[a]

[a] FiFe Batteries, E1 Culham Science Centre, Abingdon, Oxfordshire OX14 3DB, UK
[b] Chemistry Division, University of Surrey, Guildford GU2 7XH, UK

ARTICLE INFO

Article history:
Received 25 July 2008
Received in revised form 29 August 2008
Accepted 16 September 2008
Available online 7 October 2008

Keywords:
Lithium
Tungstate
Insertion
Battery
Anode

ABSTRACT

The iron tungstate materials $Fe_2W_yO_{3(y+1)}$ ($y = 1$ and 3) have been synthesized by a low temperature route, and their lithium insertion properties measured using galvanostatic and EVS measurements. This paper reports the lithium insertion into Fe_2WO_6, $Fe_2W_3O_{12}$ and nano-composite Fe_2WO_6/WO_3 materials made by this co-precipitation route. Relatively high initial discharge capacities were observed for all materials, the highest being 653.9 mAh g^{-1} for the $y = 3$ material heat treated at 500 °C. Rapid capacity fade behaviour was observed for all materials prepared at 500 °C. Improved performance was determined for the iterations heat treated at 950 °C with a reversible specific capacity of 320 mAh g^{-1} observed for the Fe_2WO_6 sample.

1. Introduction

Lithium ion batteries are a highly effective method of energy storage, and much of the current research emphasis in this area is on finding alternatives to the industry standards electrode materials, $LiCoO_2$ and graphite. Materials such as the titanate spinel ($Li_4Ti_5O_{12}$) are receiving significant attention as alternative 'safer' anodes, although a significant drawback with this approach is the higher operating voltage of around 1.5 V vs. Li. This property reduces the voltage of the resultant lithium ion cell and hence a $LiCoO_2$//titanate cell will operate at about 2.5 V, rather than around 4 V when used with a conventional graphite electrode.

Materials which possess more complex structures such as the NASICON ($Li_3Fe_2(PO_4)_3$) [1] and Garnet ($Li_5Ln_3Sb_2O_{12}$ (Ln = La, Pr, Nd, Sm and Eu)) [2] type structures possess open frameworks and flexible networks of poly anions, these structures allow fast lithium ion conduction through channels and hence potentially increase the ionic conductivities. Bruce et al. have studied sodium insertion in the defect garnet structures $Fe_2(MO_4)_3$ here M – Mo and W [3] while Manthiram and Goodenough have investigated the chemical lithiation of $Fe_2(MO_4)_3$ frameworks [4]. Montemayor et al. [5] have also looked at tungstate systems of the formula MWO_4, these materials prepared by low temperature methods show improved properties compared to high temperature solid state methods. This work investigates iron tungstate materials with the formula $Fe_2W_yO_{3(y+1)}$ where $y = 1$ and 3 (Fe_2WO_6 and $Fe_2(WO_4)_3$) synthesized by a low temperature co-precipitation routes. The $Fe_2W_yO_{3(y+1)}$ systems also exhibit higher average values vs. Li/Li+ than the standard graphite systems, this does reduce the energy density of the resulting lithium ion battery. However this higher average voltage does have the added advantage of providing a safer alternative and also raises the possibility of using high voltage materials, such as the 5 V spinels without causing thermal runaway of the lithium ion battery.

2. Experimental

2.1. Synthesis

The iron tungstate materials corresponding to general formula $Fe_2W_yO_{3(y+1)}$ where $y = 1$ and 3, were all synthesized using a low temperature co-precipitation route. In summary, on dissolving the tungstic oxide in concentrated ammonium hydroxide the colour of the agitated mixture changed from a yellow/green suspension to a white suspension, and finally to a murky, transparent solution. This corresponds to the formation of ammonium tungstate $(NH_4)_2WO_4$ which slowly dissolves to produce an ammonium tungstate solution. On addition of an alcoholic solution of iron nitrate (95% ethanol) to the tungstate solution a gelatinous dark red precipitate is produced (iron hydroxide), which upon agitation over several hours at an elevated temperature formed a homogeneous red suspension. This precipitate was then filtered washed and dried.

* Corresponding author at: FiFe Batteries Ltd, E1 Culham Science Centre, Abingdon, Oxfordshire, OX14 3DB, UK. Tel.: +44 1865408246; fax: +44 1865408249.
E-mail address: Emma.Kendrick@fifebatteries.co.uk (E. Kendrick).

0378-7753/$ – see front matter © 2008 Published by Elsevier B.V.
doi:10.1016/j.jpowsour.2008.09.103

After heating a dark red/black material was formed. The samples fired to 500 and 950 °C were chosen for further testing.

2.2. Characterisation

The composition and phase analysis of the iron tungstate materials were performed by X-ray diffraction (Siemens D5000 Cu Kα) $2\theta = 10–70°$ over a period of 1 h.

Composite electrodes were made by mixing the active material with denka black and EPDM in the ratio of 95/3/2, this mix was then coated onto a copper current collector using a micrometer blade on a paint applicator base. The resulting coating was then dried, calendared and then cut into disks. Cells for electrochemical testing were made by stacking the coated disk with a glass fibre separator and a lithium/nickel anode. The stack was placed into a soft pack cell in between two nickel tabs and then vacuum sealed before clamping and placing onto the electrochemical testing rig. An electrolyte with 1.2 mol solution of $LiPF_6$ in EC/DEC (20/80) by volume was used.

High resolution lithium insertion data were collected using the electrochemical voltage spectroscopy (EVS) technique [7]. EVS employs a voltage step protocol to provide a close approximation to the open circuit voltage titration curve for the electrochemical system under investigation. In the test in the present investigation the EVS voltage increments were 10 mV while the limiting current density was 10 mA g^{-1}.

Cycling tests were undertaken using a commercial battery cycler (Maccor Inc., Tulsa, USA). These tests were carried out at 23 °C in metallic lithium cells at a constant current density of 10 mA g^{-1} using voltage limits of 3.0 and 0.5 V vs. Li. The electrolyte was a 1 M $LiPF_6$ solution in EC/DEC/EMC 1/1/1 by volume.

3. Results and discussion

Representative iron tungstate samples were selected for X-ray diffraction and electrochemical insertion studies.

$Fe_2W_yO_{3(y+1)}$ $y = 1$ sample, synthesized using the co-precipitation method described exhibited a non-crystalline structure which crystallised to a pure Fe_2WO_6 phase upon heating to temperatures above 650 °C. The samples for further electrochemical analysis were selected from those heated to 950 °C for 6 h and 500 °C for 12 h (see Fig. 1a).

The iron tungstate material $Fe_2W_yO_{3(y+1)}$ $y = 3$ was heated at temperatures ranging from 350 to 950 °C. At 300 °C the sample was X-ray amorphous, while after heating at 500 °C for 12 h the material still appeared relatively amorphous with very broad peaks at around 20–25° 2θ. On further heating, a mix composite of WO_3 and Fe_2WO_6 was observed, possibly due to the decomposition of the non-crystalline meta stable phase, $Fe_2(WO4)_3$. Previous studies have shown decomposition to Fe_2WO_6 and WO_3 to take place at temperatures above 550 °C [6]. Samples used for electrochemical lithium insertion experiments were taken after heating to 950 °C for 6 h and 500 °C for 12 h (see Fig. 1b).

During preliminary electrochemical testing it was noted that all samples showed relatively high irreversible capacity loss on the first cycle. A summary of the first cycle capacities, 1st cycle loss, 3rd discharge capacity and capacity fade over the rest of the life of the cell are given in Table 1.

Fig. 2 depicts the first cycle EVS response for the Fe_2WO_6 ($Fe_2W_yO_{3(y+1)}$, $y = 1$) material synthesized at 950 °C. To aid clarification, it should be noted that a one-electron reduction reaction in this material corresponds to a specific capacity of 68.45 mAh g^{-1}. The first discharge process generates a specific capacity of 470 mAh g^{-1} while the subsequent charge process amounts to

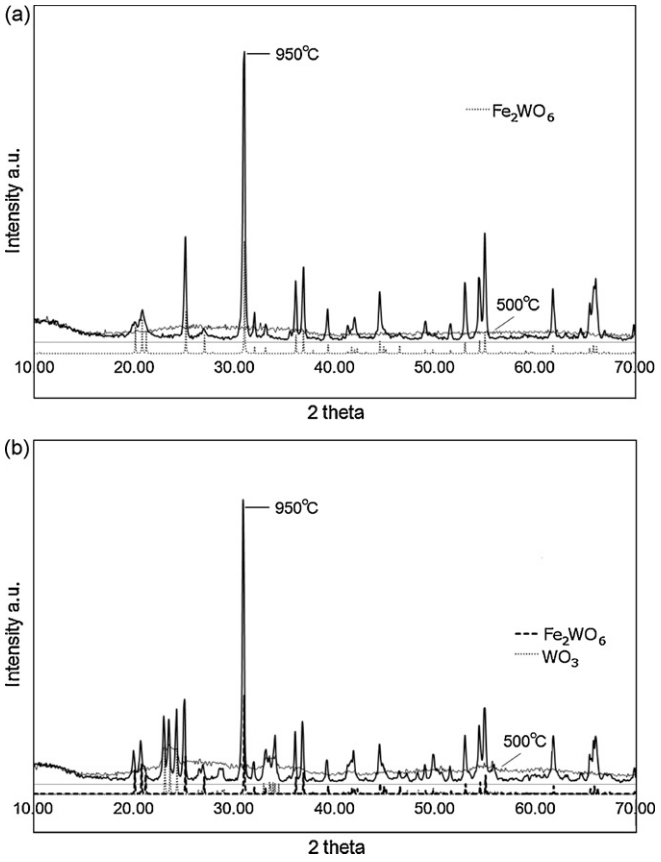

Fig. 1. (a) X-ray diffraction patterns for the material $y = 3$, heat treated to 500 and 950 °C for 6 h, together with the calculated patterns for WO_3 and Fe_2WO_6 in black and blue, respectively. (b) The X-ray diffraction pattern for the material $y = 3$ heat treated to 500 and 950 °C, with the calculated pattern for Fe_2WO_6 shown in black.

around 370 mAh g^{-1}, corresponding to a charge inefficiency of around 21%. Poor charge efficiency is relatively common in low voltage, iron-based lithium insertion systems and is associated with the poor reversibility Fe^0/Fe^{n+} redox couple [8].

As indicated in this figure, the discharge process may be separated into four, distinct voltage regions (shown as text annotation, A–D). We also denote these processes on the associated differential capacity profile. We believe that Region A is associated with irreversible charge consumption due to surface layer formation. This observation is further supported by the indistinct and noisy differential capacity behaviour which is consistent with irreversible cell reactions. This type of behaviour has been reported for lithium insertion in γ-Fe_2O_3 electrodes and has been related to reduction of Fe^{3+} surface species [9].

Region B is characterized by a voltage plateau and most likely corresponds to iron ($Fe^{3+} \rightarrow Fe^{2+}$) reduction:

$$2Li^+ + 2e^- + Fe_2WO_6 \rightarrow Li_2Fe_2WO_6(Fe^{3+} \rightarrow Fe^{2+}) \quad (1)$$

In Region C, tungsten is reduced ($W^{6+} \rightarrow W^{4+}$) by a two-electron transfer, which corresponds to the following reaction:

$$2Li^+ + 2e^- + Li_2Fe_2WO_6 \rightarrow Li_4Fe_2WO_6(W^{6+} \rightarrow W^{4+}) \quad (2)$$

Region D is characterized by a sloping voltage behaviour (and rather indistinct differential capacity response) which suggests material 'amorphotization' related to the four-electrode reduction of Fe^{2+} to metallic iron (Fe^0). The formation (extrusion) of Fe^0 will induce active material decomposition and the simultaneous isolation of

Table 1
A summary of the electrochemical performance data for the $Fe_2W_yO_{3(y+1)}$ (where $y = 1$ and 3) tungstate materials, heat treated at 500 and 950 °C.

y	Specific capacities (mAh g^{-1})					Specific capacities (mAh g^{-1})				
	500 °C					950 °C				
	1st Discharge	1st Charge	3rd Discharge	1st Cycle loss	%Loss 3D/7D	1st Discharge	1st Charge	3rd Discharge	1st Cycle loss	%Loss 3D/7D
1	555.9	302.5	193.7	45.6	63.1	485.8	376.9	337.9	22.4	8.2
3	653.9	280.2	278.9	57.1	16.0	443.9	284.7	215.2	35.9	43.4

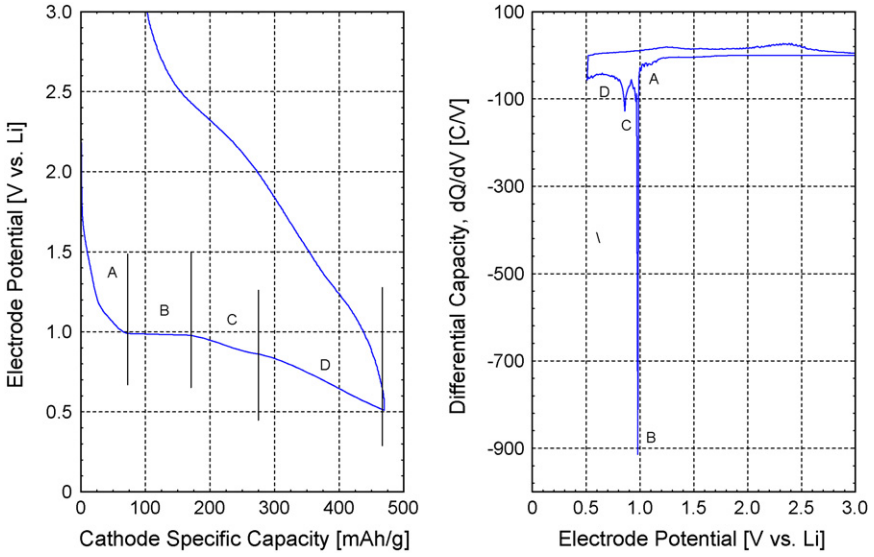

Fig. 2. First cycle EVS response for the Fe_2WO_6 sample heat treated at 950 °C, using a critical current density of 10 mA g^{-1} between voltage limits of 0.5 and 3.0 V vs. Li.

lithium oxide, Li_2O and tungsten dioxide, WO_2:

$$4Li^+ + 4e^- + Li_4Fe_2WO_6 \rightarrow 2Fe^0 + 2Li_2O + WO_2(Fe^{2+} \rightarrow Fe^0) \quad (3)$$

The amorphous properties of the reduction product are supported by the nature of the subsequent charge process which is characterized by generally sloping voltage behaviour. The differential capacity profile for this process shows two very broad peaks, centred at around 1.3 and 2.3 V vs. Li. These poorly resolved features presumably corresponding to the re-oxidation of metallic iron as well as the W^{4+} to W^{6+} transition (WO_2 to WO_3). Subsequent EVS cycling (not shown) shows poorly resolved differential capacity data for both discharge and change supporting the insertion mechanism.

The formation of amorphous phases by electrochemical lithium reduction of the Fe_2WO_6 is supported by similar studies reported for the related $Fe_2(WO_4)_3$ material [4]. Controlled chemical lithiation of this material using *n*-BuLi initially causes reduction of Fe^{3+} to Fe^{2+} followed by extrusion of Fe^0 and formation of W^{4+}(as WO_2). This reduction process results in an amorphous product in which the metallic iron forms clusters that are too small to be clearly identified by X-ray diffraction. The other products of this process are Li_2O and WO_2. The creation of small iron clusters is also consistent with similar observation reported during the chemical lithiation of the iron oxides, Fe_2O_3 and Fe_3O_4 [10].

Fig. 3 shows the preliminary constant current cycling behaviour for the Fe_2WO_6 material heat treated at 950 °C. The initial discharge specific capacity is around 380 mAh g^{-1}, broadly consistent with the EVS data shown in Fig. 2. As depicted, over the initial seven cycles the discharge specific capacity declines to 318 mAh g^{-1}, indicating a capacity fade of 16.3%.

In Fig. 4, the first cycle EVS voltage profile and differential capacity data for the Fe_2WO_6 material heat treated at 500 °C is shown. For this experimental iteration the first discharge process is equivalent to a specific capacity of 556.1 mAh g^{-1} while the subsequent charge process corresponds to 302.0 mAh g^{-1}. The first cycle charge inefficiency is around 46% which presumably reflects the low crystallinity of the as-prepared active material.

From inspection, the voltage profile for the discharge process is characterized by a general sloping behaviour, but also contains some voltage 'structure'. This is more clearly depicted in the differential capacity profile which indicates two main reduction peaks at 1.5 and 0.7 V. Allowing for voltage shift it is likely that these peaks are similar to those reduction reactions described for the material synthesized at 950 °C. Interestingly, the differential capacity profile for the subsequent charge process – characterized by broad peaks

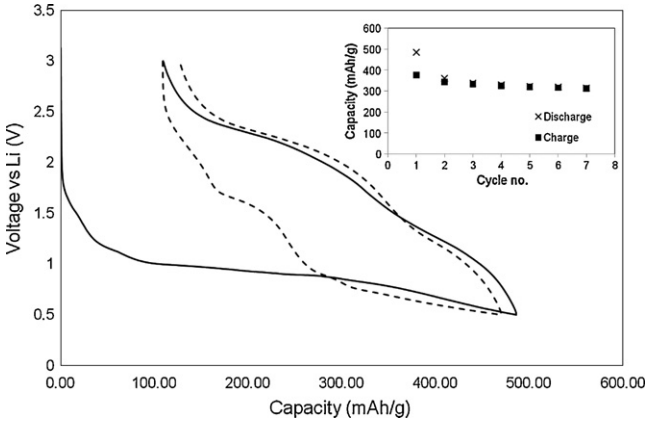

Fig. 3. First and second cycle voltage profiles and cycle data for the Fe_2WO_6 sample heat treated at 950 °C, using a constant current density of 10 mA g^{-1} between voltage limits of 0.5 and 3.0 V vs. Li.

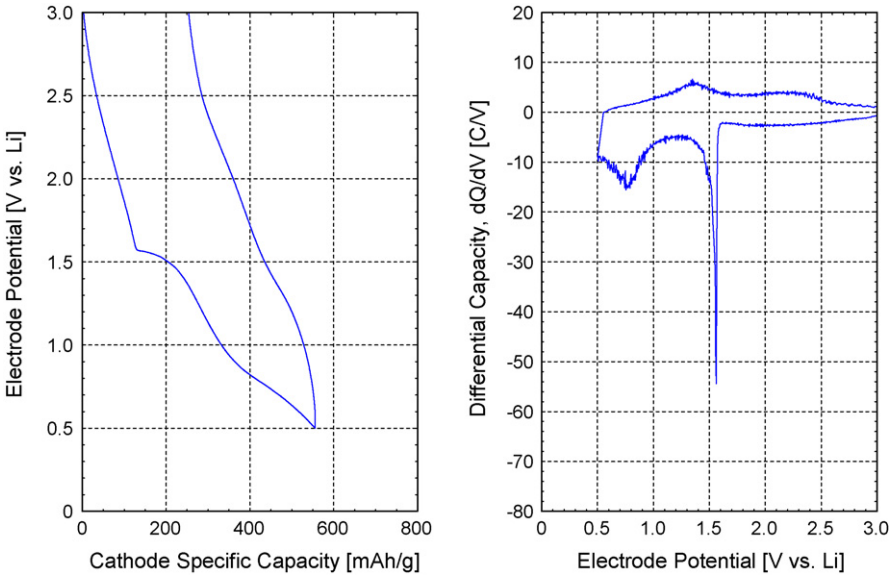

Fig. 4. First cycle EVS response for the Fe_2WO_6 sample heat treated at 500 °C, using a constant current density of 10 mA g^{-1} between voltage limits of 0.5 and 3.0 V vs. Li.

centred at about 1.3 and 2.2 V vs. Li – is broadly consistent with the data presented for the 950 °C material. This suggests the similarity in the oxidation behaviour for the two materials.

Fig. 5 shows the constant current cycling behaviour for the Fe_2WO_6 material synthesized at 500 °C. The initial discharge specific capacity is around 280 mAh g^{-1}, and during the first 12 cycles the material shows a steady and fairly rapid capacity fade. By cycle 12 the specific capacity has declined to 192 mAh g^{-1}, corresponding to an overall capacity fade of about 31% over this cycling period.

Fig. 6 shows the first and second cycle data for the $Fe_2W_yO_{3(y+1)}$ where $y = 3$ for the sample heated to 950 °C, an initial discharge capacity of 444 mAh g^{-1} is observed for this sample while the subsequent charge process is 285 mAh g^{-1}, the first cycle charge inefficiency is approximately 36%. This material is a Fe_2WO_6 and WO_3 composite and hence the first discharge capacity at 0.7 V is similar to that observed for the Fe_2WO_6 sample as expected. Upon further cycling more structure is observed in the voltage profile, with a plateau appearing in the 1.5 V region similar to that observed on the first cycle for the low temperature materials, and the second cycle for the Fe_2WO_6 material. These phenomena have been observed previously for hydrothermally produced MWO_4 materials [5] and have been attributed to the amorphous nature of the materials. In addition, poor insertion reversibility was observed for these samples.

The material $Fe_2W_yO_{3(y+1)}$ where $y = 3$ heat treated at 500 °C is amorphous in nature, and has high initial discharge specific capacity of 653 mAh g^{-1}. The first charge capacity of 280 mAh g^{-1} corresponding to a relatively large first cycle charge inefficiency of 57.1%. Capacity fade is experienced during further cycling and the reversible discharge capacity has dropped to around 200 mAh g^{-1} after 12 cycles (Fig. 7).

The sloping voltage profiles at approximately 1 V vs. Li for these $y = 3$ systems show that with subsequent cycles a step wise voltage profile with plateaus in the 1.5 and 1 V region are observed, this profile is very similar to the voltage profiles observed for the $Fe_2W_2O_6$ systems. The decomposition mechanisms occuring in the $y = 1$ materials can therefore be applied to the decomposition reactions occuring in the $y = 3$ samples detailed above. These materials show relatively broad voltage profile, the voltage range exhibited by the $n = 3$ material may cause problems when put into a real lithium ion battery system, the $n = 2$ system however shows less of a volt-

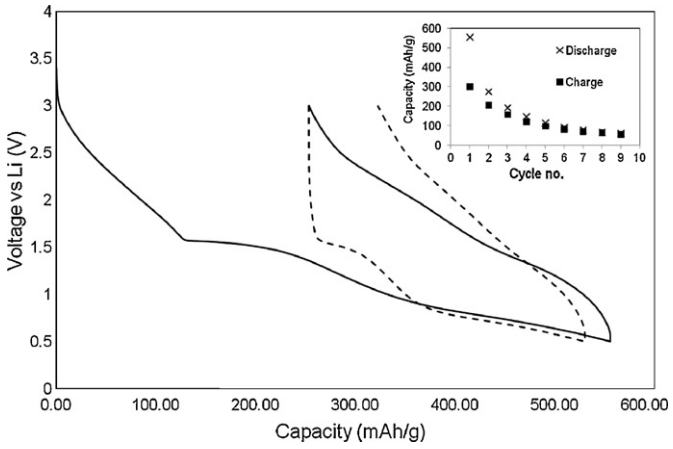

Fig. 5. First and second cycle voltage profiles and cycle data for the Fe_2WO_6 sample heat treated at 500 °C, using a critical current density of 10 mA g^{-1} between voltage limits of 0.5 and 3.0 V vs. Li.

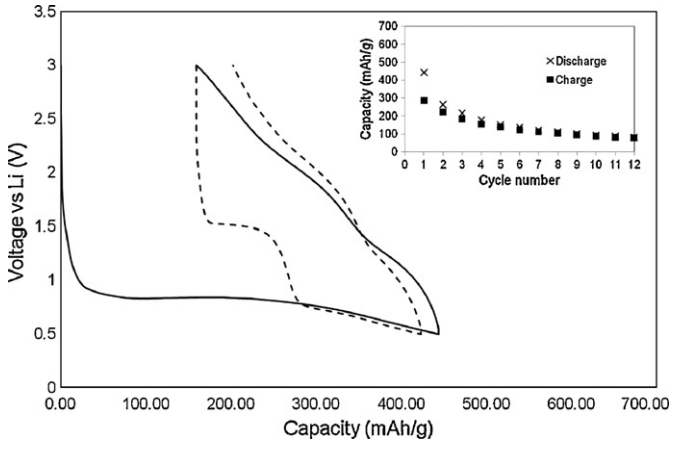

Fig. 6. First and second cycle voltage profiles and cycle data for the $Fe_2W_yO_{3(y+1)}$ $y = 3$ sample heat treated at 950 °C, using a constant current density of 10 mA g^{-1} between voltage limits of 0.5 and 3.0 V vs. Li.

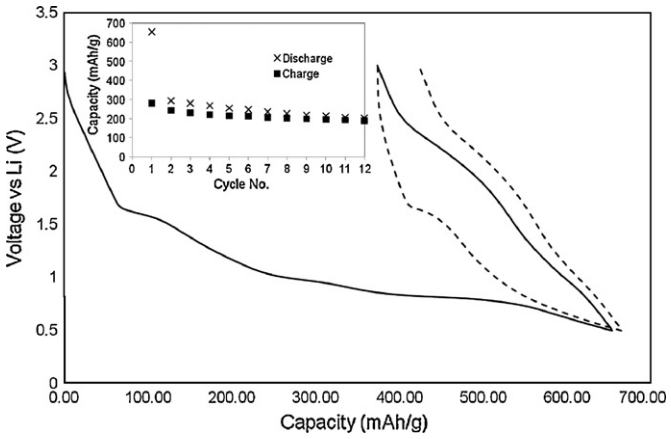

Fig. 7. First and second cycle voltage profiles and cycle data for the $Fe_2W_yO_{3(y+1)}$ $y = 3$ sample heat treated at 500 °C, using a constant current density of 10 mA g^{-1} between voltage limits of 0.5 and 3.0 V vs. Li.

age profile range vs. Li and this can be further reduced by further optimisation of the composite electrodes.

4. Conclusions

The iron tungstate materials $Fe_2W_yO_{3(y+1)}$ where $y = 1$ and 3, may be synthesized by a low temperature co-precipitation method, followed by heat treatment in the range 500–950 °C. It is found that the heat treatment temperature has a profound effect on the crystallinity and the electrochemical lithium reduction behaviour. For the case of the Fe_2WO_6 the discharge (reduction) mechanism appears to involve the initial reduction of Fe^{3+} to Fe^{2+} via a conventional lithium insertion reaction. This is followed by tungsten reduction ($W^{6+} \rightarrow W^{4+}$) and eventually (at <0.8 V vs. Li) to the 'extrusion' of metallic iron and the con-current formation of Li_2O and WO_2. These reactions are found to be only poorly reversible. It is considered likely that a similar iron extrusion reaction is occurring in the other tungstate materials. This conclusion is further supported by literature reports on the chemical reduction on the related $Fe_2(WO_4)_3$ materials [4].

References

[1] C. Masquelier, A.K. Padhi, K.S. Nanjundaswamy, J.B. Goodenough, J. Solid State Chem. 135 (1998) 228.
[2] J. Percival, E. Kendrick, P.R. Slater, Solid State Ionics 179 (2008) 1666.
[3] P.G. Bruce, G. Miln, J. Solid State Chem. 89 (1990) 162.
[4] A. Manthiram, J.B. Goodenough, J. Solid State Chem. 71 (1979) 349.
[5] S.M. Montemayor, A.F. Fuentes, Ceram. Int. 30 (2004) 393.
[6] A.K. Sriraman, A.K. Tyagi, Thermochim. Acta 406 (2003) 29–33.
[7] J. Barker, Electrochim. Acta 40 (1995) 1603.
[8] H. Morimoto, S.-I. Tobishima, Y. Lizuka, J. Power Sources 146 (2005) 315.
[9] M. Quintin, O. Devos, M.H. Delville, G. Campet, Electrochim. Acta 51 (2006) 6426.
[10] M. Thackeray, W.I.F. David, J.B. Goodenough, Mater. Res. Bull. 17 (1982) 785.